Single-Walled Carbon Nanotube Networks

Single-Walled Carbon Nanotube Networks: The Influence of Individual Tube–Tube Contacts on the Large-Scale Conductivity of Polymer Composites

*Oana A. Bârsan, Günter G. Hoffmann, Leendert G. J. van der Ven, and Gijsbertus de With**

Over two decades after carbon nanotubes started to attract interest for their seemingly huge prospects, their electrical properties are far from being used to the maximum potential. Composite materials based on carbon nanotubes still have conductivities several orders of magnitude below those of the tubes themselves. This study aims at understanding the reason for these limitations and the possibilities to overcome them. Based on and validated by real single-walled carbon nanotube (SWCNT) networks, a simple model is developed, which can bridge the gap between macroscale and nanoscale down to individual tube–tube contacts. The model is used to calculate the electrical properties of the SWCNT networks, both as-prepared and impregnated with an epoxy-amine polymer. The experimental results show that the polymer has a small effect on the large-scale network resistance. From the model results it is concluded that the main contribution to the conductivity of the network results from direct contacts, and that in their presence tunneling contacts contribute insignificantly to the conductivity. Preparing highly conductive polymer composites is only possible if the number of direct, low-resistance contacts in the network is sufficiently large and therefore these direct contacts play the key role.

1. Introduction

Electrically conductive composite materials are of interest for both research and industry due to their well-known advantages of combining the properties of individual components in one material, as well as increasing demands for flexible, strong, light, and even transparent electronics. Carbon nanotubes (CNTs) are promising as filler particles because of their high aspect ratio combined with good mechanical, electrical, and thermal properties.[1–4] However, although percolation thresholds as low as 5.2×10^{-5} have been achieved,[5] no composite is known where the conductivity reaches its maximum potential, namely that of the associated CNT network. Usually, the composites barely reach a few hundred S/m regardless of the amount of filler particles in the material,[6–8] while pure CNT films can have conductivities in the range of 10^5–10^6 S m^{-1}.[9,10] All these composites also show an increasing degree of agglomeration with increasing CNT content,[5,11,12] emphasizing the physical limitations that are associated with a higher amount of filler particles in the composite. On top of that, composites are typically prepared by adding CNTs into a polymer, either directly or by first dispersing them into water/solvents using surfactants/dispersing agents.[13–15] A major separation/stabilization mechanism for these dispersions is CNT polymer wrapping,[16–18] which leads to the presence of insulating layers surrounding the tubes. This eventually leads to high resistance tunneling contacts between the tubes in the final composite.[19–21] Therefore, as long as the goal is achieving highly conductive composite materials, there are fundamental limitations in the typical preparation approach, and composites prepared this way are not likely to ever reach their maximum potential.

Li et al.[22] used a new approach to prepare single-walled carbon nanotube (SWCNT) composite materials, a technique involving two main steps: i) preparing a uniform SWCNT thin film on a glass substrate; ii) filling the gaps between the tubes with a specific polymer, followed by drying/curing the polymer. This approach brings the advantage of ensuring a SWCNT network with good physical and electrical contacts from the beginning. In previous work,[23] we improved and adapted this technique for an epoxy-amine polymer matrix, and developed a method for large-scale in situ resistance measurements that allowed us to have direct access to the conductive network during the polymer impregnation process. The results showed that the cross-linked polymer matrix alone can lead to about 40% increase in the SWCNT network resistance, similar to the effect of liquid infiltration in carbon nanotube fibers.[24] These studies show that there are possibilities for composites to reach their maximum potential, but they do not explain what

O. A. Bârsan, Dr. G. G. Hoffmann, L. G. J. van der Ven, Prof. G. de With
Laboratory of Materials and Interface Chemistry
Department of Chemical Engineering and Chemistry
Eindhoven University of Technology
Het Kranenveld 14
5612 AZ, Eindhoven, The Netherlands
E-mail: g.dewith@tue.nl

DOI: 10.1002/adfm.201600435

happens at the nanoscale, i.e., we still do not know how the polymer affects the individual tube–tube contacts inside a composite, and how this reflects on the large-scale electrical properties of the final material. Answering these questions could lead to a general approach for preparing composite materials as conductive as their filler particles.

This study aims at understanding the effect of a polymer matrix on a SWCNT network at the nanoscale, and how this correlates with the large-scale network resistance, by combining and comparing experimental results with theoretical considerations. A simple, basic model was developed, based on and validated by real samples, which shows the dramatic effect a few tube–tube contacts can have on the large scale network resistance.

2. Results and Discussion

2.1. SWCNT Networks: Before Polymer Impregnation

2.1.1. Experimental Results

SWCNT films with a thickness range of 10–140 nm were prepared on glass substrates from SWCNT/carboxymethylcellulose (CMC) solutions, as described by Bârsan et al.[23] Two additional types of films were prepared via consecutive coating/drying cycles, with the final thicknesses of 2 and 5 µm, respectively. These last two films could easily be removed from the glass substrates and used further as freestanding SWCNT films. Transmission electron microscopy (TEM), scanning electron microscopy (SEM), and atomic force microscopy (AFM) measurements showed that the films are composed of randomly dispersed SWCNTs and ropes of aligned SWCNTs with a diameter in the range of 1–20 nm.[23] The density of the 2 µm thick films was determined by weighing a total of six samples with the dimensions: 1 cm × 1 cm × 2 µm. The calculated film density of 1.1 ± 0.1* g cm^{-3} (*standard deviation of the population) is somewhat lower than the measured densities of SWCNT bundles of 1.2–1.8 g cm^{-3},[25,26] and approximately three times lower than the calculated densities of individual SWCNTs of 3.1–3.5 g cm^{-3}.[26,27] Using a density of 1.1 g cm^{-3}, the SWCNTs occupy 61% of the film volume.

The thin films, however, are not freestanding, the weight of the CNTs is extremely small compared to the glass substrate and there are significant losses during sample pretreatments. Hence, any attempt to weigh these thin films is extremely unreliable. Therefore, a series of six individual dispersions in the range of 0.01%–0.125% SWCNTs were prepared and the absorbance of the solutions was measured at 550 nm (**Figure 1**). The results were used to calculate the density of the films with the same absorbance by "shrinking" the thickness of the cuvette with a known solution to the thickness of the corresponding SWCNT film. The calculations were done assuming that the same amount of SWCNTs absorbs the same amount of light, despite different tube orientations and scattering effects in solutions and films. The density of the thin films so obtained was 1.5 ± 0.2* g cm^{-3} (*standard deviation of the population), a value higher than the 1.1 g cm^{-3} obtained for the 2 µm thick film. This can be related to the assumptions made when

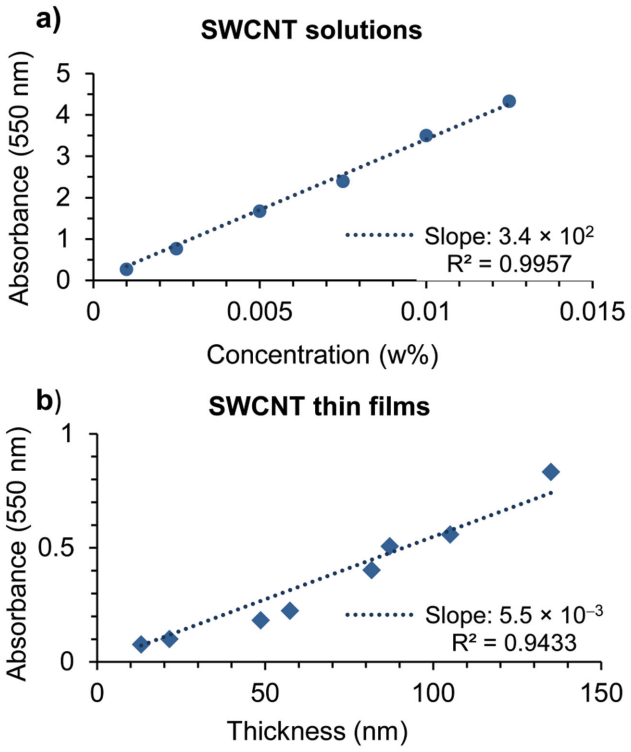

Figure 1. Absorbance ($A = -\log T$ with T the transmittance) of a) different concentration SWCNT solutions and b) different thickness SWCNT films.

applying this method, and the thin films' preferential in-plane orientation, perpendicular to the light source direction. Due to this orientation, the thin films are expected to show a higher absorbance than the same amount of carbon nanotubes randomly dispersed in water. In a previous study,[23] the SWCNT films were shown to form occasional large ropes of entangled SWCNTs at the surface, as high as 100 nm. These ropes hardly contribute to the average thickness of the thin films, but they can significantly increase their absorbance. This effect will also lead to higher density values for the thin films, when calculated based on their absorbance. Despite possible errors, the similarity between the two densities implies that there are no major differences between the thin and the thick films, supporting the idea that the thick and thin SWCNT films behave similarly upon polymer impregnation.

The large-scale resistance of all SWCNT films was measured using a four-point probe system. The values fall within the range of 4 to 1.5 × 10^3 Ω for the thickest film (5 µm) and the thinnest film (13 nm), respectively. However, SWCNTs are susceptible to chemical doping[28] upon different gas exposures[29,30] which can cause significant changes in their electrical properties. A series of consecutive heating/cooling cycles was performed on a reference sample in a nitrogen atmosphere, to determine the effect of exposure to environmental conditions on the resistance of the SWCNT films (**Figure 2**). The sample was kept at a constant temperature of 100 °C after heating and before cooling during each cycle. This was done in order to simulate the conditions needed for cross-linking the polymer mixture used in the second part of the study. Results showed that the film resistance continuously increases upon

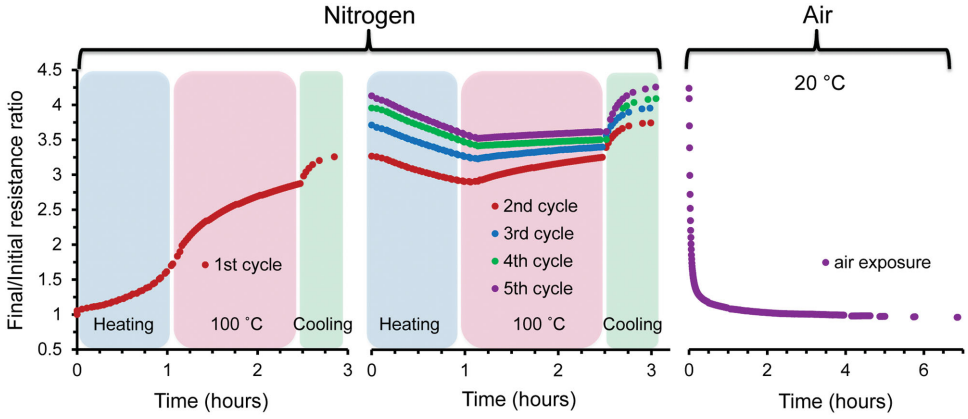

Figure 2. SWCNT network resistance upon consecutive heating/cooling cycles in a nitrogen atmosphere and subsequent exposure to environmental conditions.

heating and even continues to increase at constant high temperature due to dedoping, but reaches a consistent and typical semiconducting behavior after several heating/cooling cycles in an inert atmosphere. Upon air exposure the sample resistance drops down to the initial value, confirming that the doping/dedoping process is quantifiable and reversible.

2.1.2. Network Model

Considering that the SWCNTs in a film are all randomly stacked on top of each other with an in-plane orientation, and that the charge carriers choose the lowest resistance path possible through a film, a simple model was developed for the smallest possible SWCNT unit layer (UL) (**Figure 3**). In order to achieve this, we used the following data. The equilibrium distance between two SWCNTs is 3–3.6 Å for parallel tubes,[31–35] and 2.8–2.9 Å for crossed tubes,[36,37] with variations depending on tube diameter and the crossing angle. Because our SWCNT films consist of randomly aligned and crossed tubes, a value of 3 Å was taken as equilibrium distance between any two SWCNTs in "direct" contact (Figure 3). Using 1 nm as tube diameter (see the Supporting Information), 3 Å as tube–tube (wall to wall) distance and 2 µm as tube length, a UL network was defined with size $2 \times 2\ \mu m^2 \times 1.3$ nm. From the network density of 1.1 g cm^{-3}, an average value of $n_{UL} = 1.4 \times 10^3$ SWCNTs for a unit layer UL was calculated (see the Supporting Information). This number is lower than the theoretical maximum of 1.6×10^3 tubes, which is consistent with the fact that in practice, the tubes are not perfectly well packed due to entanglements in the network (for details, see the Supporting Information).

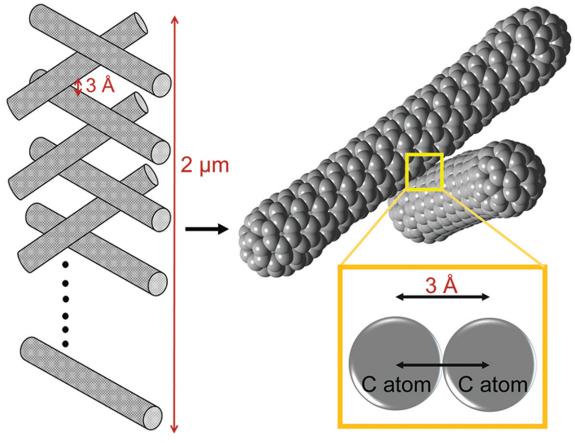

Figure 3. Schematic of a SWCNT unit layer and a direct tube–tube contact for a film of 2 µm thickness.

Due to the very large aspect ratio of the SWCNTs, the unit layer behaves like a network of resistors connected in parallel. Each SWCNT is a resistor by itself with an intrinsic resistance of 1–30 kΩ,[38–41] values that are close to the theoretical predictions of 6.5 kΩ in case of ballistic transport.[38,39] The average value of 15 kΩ was chosen as the intrinsic resistance of one individual SWCNT. However, it is usually considered that the contact resistances between the tubes play the dominant role in such a network. These contact resistances have been found to be in the range of values from tens of kΩ to several MΩ,[42–44] because SWCNTs have a wide chirality range with electronic properties from semiconducting to metallic. There are also difficulties separating the contact resistance between individual CNTs from the contact resistance between tubes and the metal electrodes used for the measurements (as the latter normally have values in the same wide range[42,45–47]). SWCNTs are also sensitive to temperature, atmosphere, doping, etc., which can all strongly influence their contact resistance. Znidarsic et al.[48] found that at ambient temperature and pressure, SWCNTs and small bundles of SWCNTs with diameter smaller than 6 nm show a reasonably narrow range of 30–530 kΩ for the contact resistances. These authors emphasize the difference between two types of contacts, namely Y-shaped contacts for which one part of a particular CNT is parallel to another CNT, and X-shaped contacts where two CNTs just cross, with Y-shaped contacts having on average a three times lower contact resistance than X-shaped contacts. This study is particularly realistic and applicable because any SWCNT dispersion or network is a mixture of individual and small bundles of SWCNTs as well as contains different types of geometrical contacts. Similar value ranges were also obtained by Nirmalraj et al.,[49] despite opposing conclusions regarding contact resistance variation

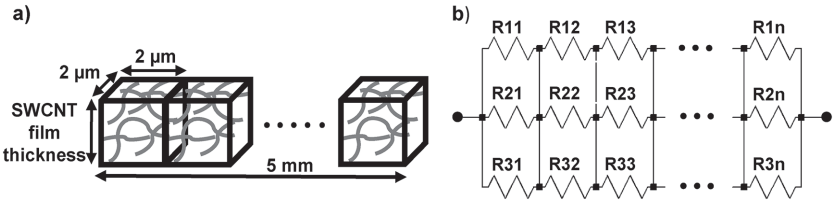

Figure 4. Schematic of a) one row of UBs connected in series across a distance of 5 mm, and b) an electrical equivalent for a network comprised of three parallel rows of UBs across a distance of 5 mm ($n = 2.5 \times 10^3$). All resistors have the same resistance, as calculated for one UB (fully comprised of either X- or Y-type contacts).

with bundle diameter. The average values of 180 kΩ for X contacts and 58 kΩ for Y contacts were used as reference for tube–tube contact resistances.[48] Because it is fairly difficult to estimate the number of X and Y contacts in a random network, the contacts were considered to be either all X-shaped or all Y-shaped, thereby defining an upper and lower range value.

Based on n_{UL} SWCNTs connected in parallel in a unit layer, the resistance for Z-type contacts (Z = X or Y) of the unit layer can be calculated via:

$$\frac{1}{R_{UL}(Z)} = \frac{n_{UL}}{R_{contact}(Z) + R_{intrinsic}} \quad (1)$$

Using $n_{UL} = 1.4 \times 10^3$, we obtain $R_{UL}(X) = 1.4 \times 10^2$ Ω and $R_{UL}(Y) = 53$ Ω, respectively.

The same type of calculations can be done for a unit block (UB), i.e., a SWCNT network comprised of a block with $2 \times 2 \times t$ µm^3, where 2 µm is the full length of a tube and t the thickness of the SWCNT film. For a film with $t = 2$ µm, this UB contains $n_{UB} = 1.9 \times 10^6$ tubes. All these tubes are considered to be connected in parallel because the length of the SWCNTs and the high network density, make it almost impossible for a tube to have only one single connection, direct or indirect, with another tube. The resistance of the UB is than given by

$$\frac{1}{R_{UB}(Z)} = \frac{n_{UB}}{R_{contact}(Z) + R_{intrinsic}} \quad (2)$$

and we obtain $R_{UB}(X) = 1.04 \times 10^{-1}$ Ω and $R_{UB}(Y) = 3.9 \times 10^{-2}$ Ω, respectively.

For our large scale, four-point probe resistance measurements, the distance between the electrodes is 5 mm. This means that 2.5×10^3 UBs fit between two consecutive probes. Because one block in the model accommodates full length carbon nanotubes, its connection to the next block will happen at the end parts of the tubes, making them connected in series (**Figure 4**a). Consequently, the large scale film resistance across a 5 mm distance was calculated as: $R_{film}(X) = 2.6 \times 10^2$ Ω and $R_{film}(Y) = 98$ Ω. Because the probes have a 0.25 mm radius spherical tip (based on the manufacturers specification), the apparent contact area between a probe and the SWCNT film will be larger than the 4 µm^2 surface area of one UB. Hence, the probe is in direct contact with more than just one UB, implying for the model that the conducting path between two consecutive probes contains several parallel rows of UBs (Figure 4b). Therefore the network resistance across a 5 mm distance was also calculated for a varying number of parallel rows of UBs (as shown in **Figure 5** for a network containing only X-shaped contacts) (see for details the Supporting Information). The same method was used to calculate the large scale resistances of SWCNT films with thicknesses between 10 nm and 5 µm. Note that the UB size is always $2 \times 2 \times t$ µm^3, where t is the film thickness.

Before comparing the model results with the experimental data, a dedoping correction factor was applied for the latter, based on previous experiments (Figure 2), because doping is a factor not considered in the model. The comparison between the model data and the experimental results indicates that they compare rather favorably, showing virtually the same dependence on thickness (Figure 5). Also the overall level is matching well using about seven parallel rows of UBs.

To put the result in perspective, in reality there is, of course, no such clear distinction between one UB and another, but the network density and the type of contacts between the SWCNTs, geometrical and electrical (in parallel or series), are the same. Moreover, it is difficult to estimate the real contact area between the electrodes and the SWCNT film and the model provides an estimate for the effective contact width (area) of about 14 µm (28 µm^2), which is not unreasonable in view of the size of the electrodes. Evidently, the network model is a simple one and assumes that there is only one contact point between two consecutive SWCNTs in a unit layer, but probably, due to the ability of the SWCNTs to entangle with each other, more contact points are present between tubes. Although this affects the final contact configuration, the large number of contacts will still lead to a well-determined effective contact resistance. Also the length and diameter of the real SWCNTs are variable leading to variations in the number of tubes and contacts within a UB. The model uses average contact resistance and intrinsic resistance values from literature, while in reality we have a random mixture of SWCNTs with different chirality and different electrical properties. This can lead to significant differences in intrinsic and contact resistances from one tube to another, and it would be impossible to choose one value to fit all. Despite

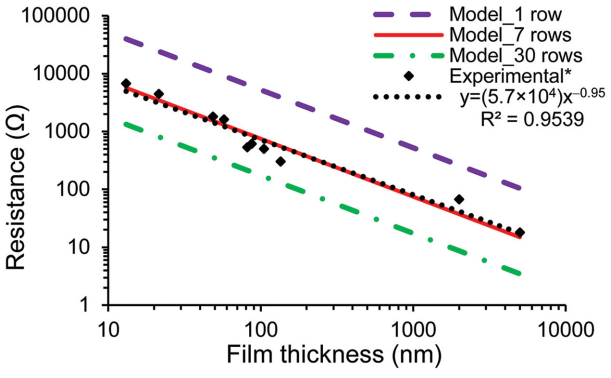

Figure 5. Resistances of different thickness SWCNT films obtained via four-point probe measurements (*dedoped) versus network model calculations for networks with 1, 7, and 30 parallel rows of UBs containing only X-shaped contacts. Similar results were obtained for networks containing only Y-shaped contacts (see Figure S4 in the Supporting Information).

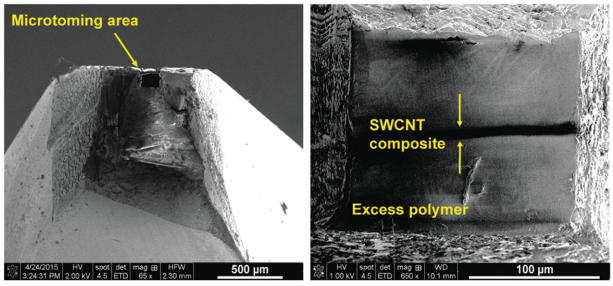

Figure 6. SEM images of an SWCNT composite film imbedded in an epoxy-amine polymer matrix.

all simplifications, the model fits well with the experimental results and shows the same behavior as the experimental data, showing that the simple network model developed can be used to calculate reasonable and realistic network resistances at a small scale as well as at a large scale.

2.2. SWCNT Networks: After Polymer Impregnation

2.2.1. Experimental Results

Pieces of 4×8 mm^2 were cut from a freestanding SWCNT film with a thickness of 2 µm, placed in silicone molds and impregnated with an epoxy-amine polymer mixture under vacuum. These samples were then cured at 100 °C for 4 h, removed from the molds and prepared for ultramicrotoming (**Figure 6**).

SEM and AFM images were taken at the cross-section of the polymer imbedded composite film, on bulk samples (Figure 6) as well as on microtomed sections (**Figure 7**b), to verify that there are no air bubbles or inhomogeneities in the newly formed composite. Systematic SEM measurements were done using a viewing orientation normal to the SWCNT film cross-section to determine the precise thickness of the SWCNT film before (Figure 7a) and after polymer impregnation (Figure 7b). For the pure SWCNT film, measurements were done on an edge obtained by cutting with scissors as well as on an edge obtained by manual breaking. The thickness of the SWCNT composite film was determined from multiple measurements on sections with 100 and 200 nm thickness. These results were also verified by AFM measurements on the bulk sample (Figure 6) and TEM measurements on 100 nm sections. All these results indicate that the composite film has a thickness ≈15% higher than the initial pure SWCNT film. This thickness increase is further denoted as swelling.

2.2.2. Network Model

Dividing the 15% swelling (i.e., 0.31 µm thickness increase for the 2.03 µm thick film) by the average number of 1.4×10^3 contacts obtained for our UL, an average distance of 2.2 Å between each two consecutive SWCNTs can be calculated. This value represents the thickness of the insulating layer formed between each two tubes in contact and the tunneling distance of that specific contact. However, the amine molecular chain can be as wide as 3.5 Å while the epoxy molecular chain can be as wide as 5 Å (without including steric effects). Even assuming that due to possible π–π stacking, the benzene rings would align with the surface of the SWCNTs, their van der Waals thickness is still 3.4 Å,[50,51] and not likely to fit in. Unfortunately, the thickness of the polymer layer between all contacts cannot be measured, and precise estimates on how the polymer chains can arrange themselves around the tube walls are fairly difficult. It is also not realistic to assume that the polymer creeps in between all

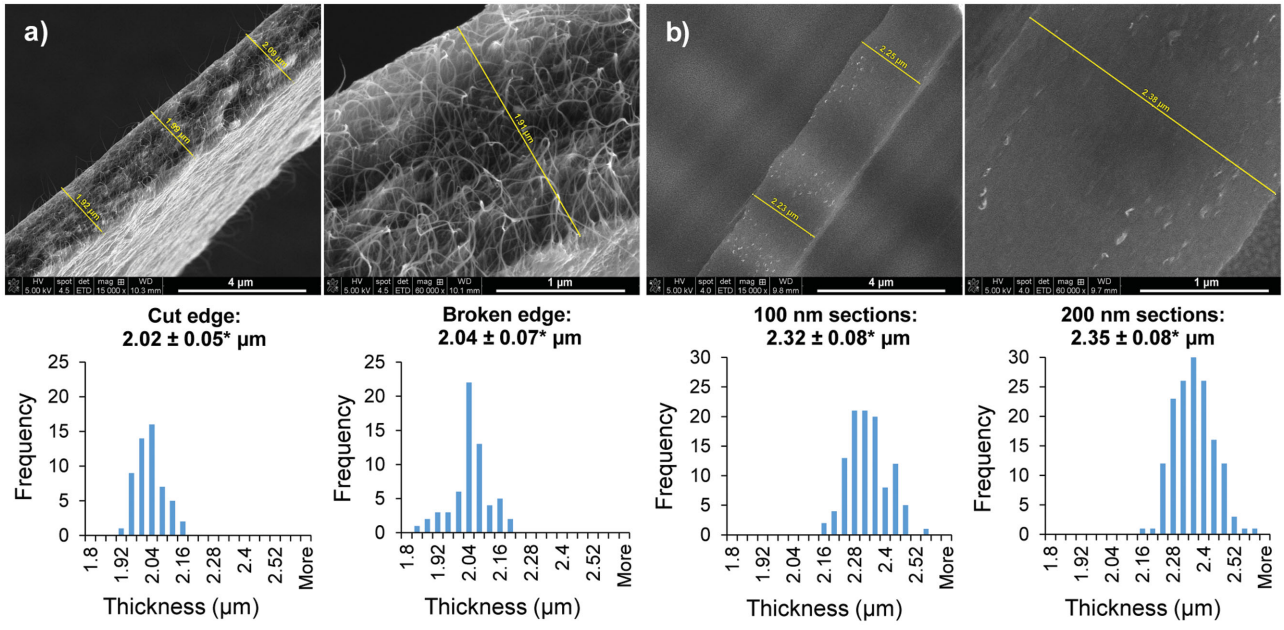

Figure 7. SEM images and thickness histograms of 2 µm SWCNT film a) before and b) after polymer impregnation with an epoxy-amine polymer (*standard deviation of the population).

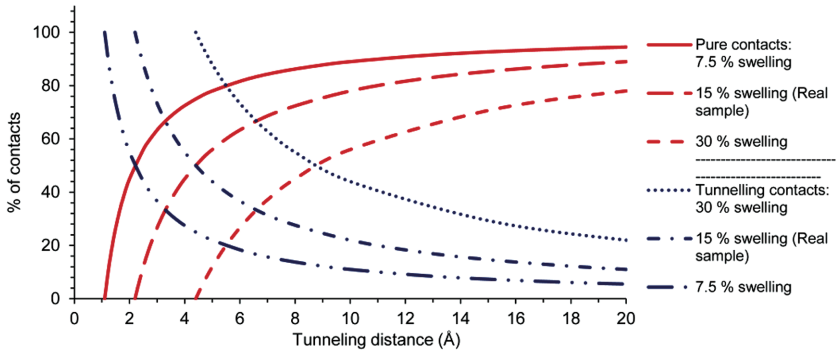

Figure 8. Percentage variation of direct/tunneling contacts as a function of tunneling distance for different swelling degrees.

contacts in the same way. Therefore we took into consideration different possibilities based on either of the two assumptions:

1. All the contacts get a 2.2 Å insulating layer upon polymer impregnation, implying that all contacts in the UB have the same tunneling distance and resistance;
2. Only some contacts get an insulating layer while the rest remain unchanged (direct contacts), implying that the additional 15.2% in film thickness has to be distributed only over the tunneling contacts. Because there is no way to verify how many tunneling and how many direct contacts we have, their numbers were systematically varied, while maintaining the total number of 1.4×10^3 contacts constant. Note that the percentage of tunneling/direct contacts also changes for different tunneling distances. **Figure 8** shows how these percentages vary with the tunneling distance for different swelling degrees.

The tunneling resistance depends not only on the thickness of the insulating layer, but also on the nature and properties of both the SWCNTs and the polymer matrix. Previous studies have shown that the tunneling resistance between two SWCNTs with an epoxy layer of ≈4 Å in between is $R_{tunneling} = 10^7$–10^9 Ω.[19,20] These values are 5–7 orders of magnitude larger than the contact resistances of direct contacts. Despite experimental difficulties and errors, Wold et al.[52] showed that there is a difference between the tunneling resistance, e.g., a 4 Å layer of unsaturated molecules ($R_{tunneling} < 10^5$ Ω) and saturated molecules ($R_{tunneling} > 10^5$ Ω), and this difference becomes more significant for tunneling distances above 5 Å. The tunneling resistance values for epoxy polymers determined by Li et al.[19] and fitted by Ward[53] were used to calculate the resistance of the tunneling contacts in our model. The maximum insulating layer between two contacting tubes was taken as 2 nm, because for larger values tunneling is considered to have a negligible contribution to the electrical transport.[54,55]

The results of the model calculation (**Figure 9**) show that the network resistance gradually increases with tunneling distance until it reaches a maximum, after which the network resistance starts to decrease. The maximum value occurs at a tunneling distance of 3.5 and 3.2 Å for X- and Y-types of contacts, respectively, regardless of the percentage of tunneling contacts. At these values, the tunneling resistances are, respectively, 11 and 12 times higher than the direct contact resistance for X- and Y-types of contacts. For tunneling distances smaller than the maximum values, the reliability of the tunneling resistance values is questionable because of the physical limitations that come with the dimensions of the real polymer chains. At these distances it is possible that the polymer simply pushes contacting SWCNTs apart without necessarily creeping in between the tubes. In this case, there is still tunneling between the tubes, but tunneling through air/vacuum. Choosing where to draw the line is difficult, but since a smaller dielectric constant of the insulating film leads to a lower tunneling resistance,[56] the fact that the network resistances would be lower for tunneling through air/vacuum is easy to foresee.

The SWCNTs are randomly oriented in the network and entangled with each other so there are different possible tunneling paths and distances for each individual contact. Because of the exponential distance dependence of tunneling, the current tends to follow the shortest path possible from one tube to another, which is normal to the tubes,[57] thus reducing the probability of other potential tunneling paths in one contact to a minimum. However, our model uses a constant tunneling distance and consequently a constant resistance for all tunneling contacts in the network, which is not representative for real samples. In order to assess how this simplification affects the network behavior, a two-parameter Weibull distribution $f(x;a,\beta) = \frac{a}{\beta^a} x^{a-1} e^{-\left(\frac{x}{\beta}\right)^a}$ was applied for all tunneling distances of the tunneling contacts in the network. Results show that using these distributions only the height of the maximum is slightly changed and that the general network behavior remains the same (Figure 9). Our previous in situ resistance measurements showed an about 40% resistance increase of the SWCNT network due to the polymer impregnation alone.[23] This value fits well into the resistance range calculated using the model (dotted lines in Figure 9).

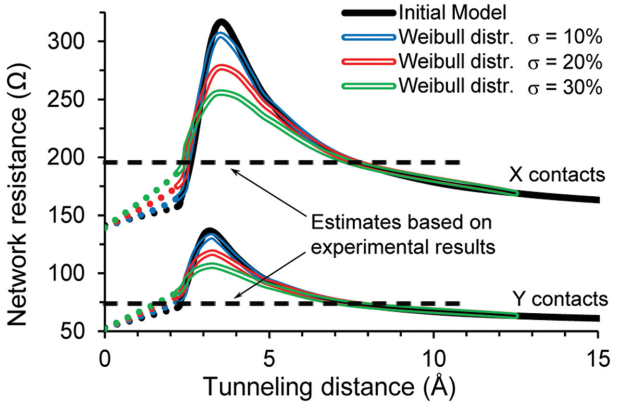

Figure 9. Resistance of the UL for constant tunneling distances (initial model) and for tunneling distances with Weibull distributions for different standard deviations (σ).

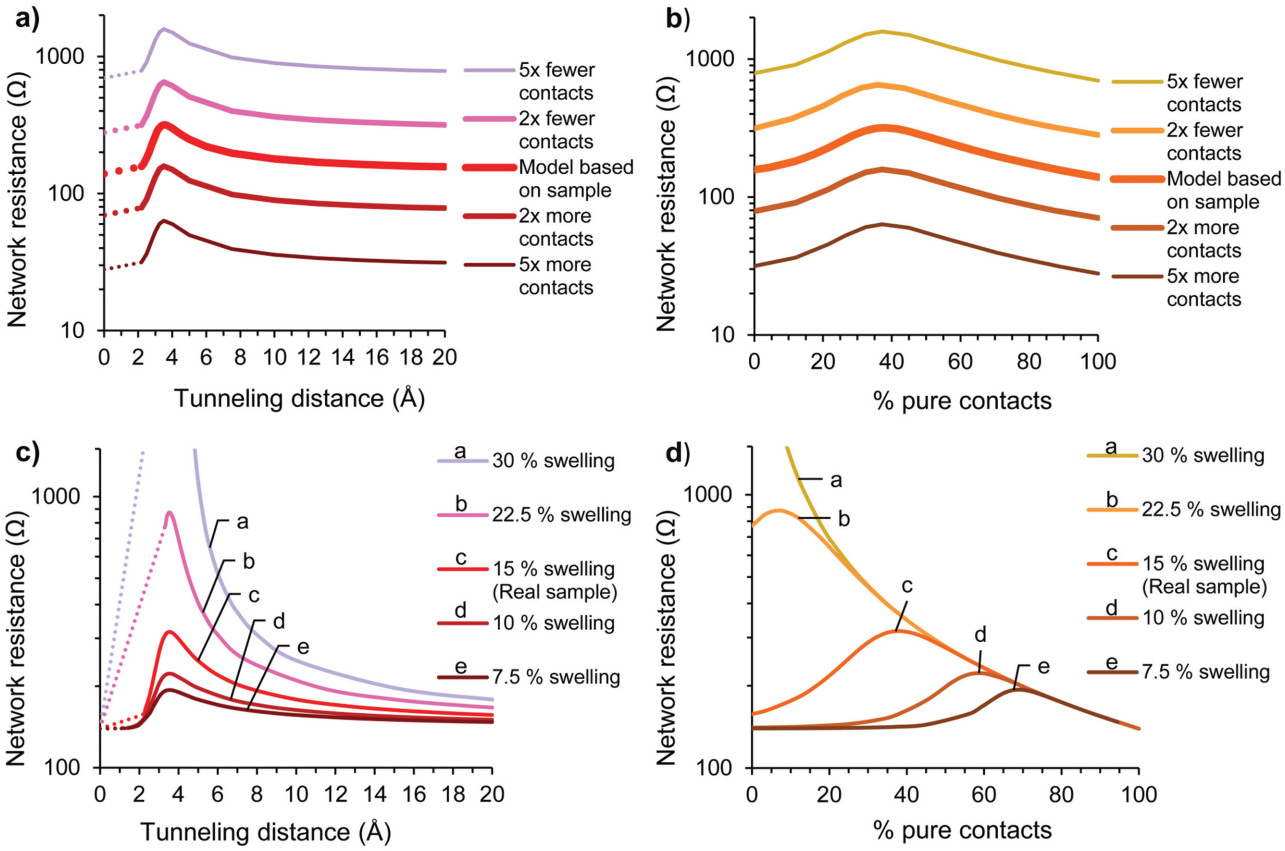

Figure 10. Resistance of a UL containing only X-shaped contacts with a,b) varying number of contacts and c,d) varying swelling degrees. Similar results were obtained for a UL containing only Y-shaped contacts (Figure S5, Supporting Information).

In order to assess whether our results show general network behavior or whether they fit our model system only, the same calculations were done while varying the number of contacts in the network model and the thickness increase. By changing the number of contacts in the network model while maintaining the 15.2% swelling constant (**Figure 10**a,b), no difference was observed in the behavior of the network resistance with regard to the number and type of contacts or even tunneling distance. The only difference from one model to another is the systematic resistance decrease with an increasing number of contacts. By changing the swelling percentage due to polymer impregnation while maintaining the number of contacts constant, the percentage of tunneling and direct contacts is also changing with the tunneling distances (Figure 8). The values of the maximum network resistance are at the same tunneling distances, regardless of swelling degree and the percentage of pure/tunneling contacts (Figure 10c,d). These results confirm that the 3.5 Å tunneling distance actually acts as a threshold. For distances smaller than this threshold, the network resistances are constantly increasing with the tunneling distance, while for distances larger than the threshold, the network resistance values are virtually identical at the same percentages of direct contacts for all swelling degrees and are (mainly) determined by the direct contacts alone (Figure 10d). This shows that for distances larger than the threshold, tunneling resistances are too high and no longer contribute to the network conductivity, and only the direct contacts determine the electrical transport in the network. The same calculations were done for networks containing only Y-type of contacts (Figure S6, Supporting Information) and they showed exactly the same type of behavior, but with the threshold (maximum resistance peak) at 3.2 Å.

3. Conclusions

We have used experimental results to develop and validate a simple model to describe SWCNT networks, both for as-prepared networks and networks impregnated with an epoxy-amine polymer. While the experimental results show the large-scale physical and electrical properties of the networks, the model provides an insight on which contacts contribute to the conductivity. The model shows that after impregnating an existing SWCNT network with a polymer, there is a threshold for tunneling distances above which the tunneling contacts no longer contribute significantly to the network conductivity. While the precise value of the threshold may be specific for our model and may change for other polymers, conductive particles or conditions, the model provides a useful tool to explain why the polymer impregnation process had such a small effect on the large-scale resistance of our SWCNT films. More explicitly, already a small tunneling distance between two CNTs can lead to a negligible contribution to the composite conductivity.

This is why, even after the percolation threshold is reached in a typical composite material, the conductivity does not increase significantly with the addition of more filler particles. It is still the presence of a relatively small number of good contacts that ensures conductivity, rather than the total number of filler particles. It is "quality-over-quantity" put into practice. Moreover, the typical methods of preparing electrically conductive composite materials by dispersing the filler particles in a polymer matrix generally lead to much larger tunneling distances than 3.5 Å, making the addition of increasing amounts of filler particles almost fruitless from the electrical point of view. Our results suggest that in order to achieve highly conductive composite materials, the preparation process needs to be approached from a different perspective, for example, by using preprepared CNT networks. They also show that it is possible to prepare composites (nearly) as conductive as their filler particles, but that ensuring the presence of low-resistance contacts between the particles is essential.

4. Experimental Section

SWCNT Solutions and Films: SWCNT films were prepared as described in Bârsan et al.[23] from 0.1% SWCNT dispersions with a SWCNT/CMC ratio of 1/30. The two thicker films of 2 and 5 µm, were prepared from a 0.2% dispersions of SWCNTs with a SWCNT/CMC ratio of 1:20. After sonication and centrifugation, the dispersions were deposited on 7×7 cm^2 glass substrates with a 250 µm gap doctor blade at a speed of 10 mm s^{-1}, using a COATMASTER 509 MC. The samples were then dried for 5 min at 45 °C under vacuum, and the coating/drying cycle was subsequently repeated 16 and 40 times, respectively. The final samples were then dried for 20 h at 45 °C before being subjected to the same acid and thermal treatment as the previous samples.[23] SEM images were taken with a Quanta 3D FEG microscope to determine the thickness of the resulting freestanding SWCNT films.

Another series of eight individual dispersions were prepared in the range of 0.01%–0.125% SWCNTs (with a SWCNT/CMC ratio of 1:30), following the same sonication and centrifugation procedures. These dispersions were diluted ten times and absorbance measurements were taken at 550 nm in 1 cm thick quartz cuvettes using an Ocean Optics USB 4000 spectrophotometer with a deuterium light source.

Resistance Measurements: Sheet resistance measurements were performed using standard four-point probe measurements with 0.5 mm diameter electrodes with a cone-shaped tip and 5 mm probe spacing. A Keithley electrometer model 6517A and source-meter model 237 were used to apply current and measure the resulting voltage drop. The results were converted to sheet resistance using correction factors for rectangular thin films as shown by Smits et al.[58] The heating/cooling cycles to determine the effect of doping on the resistance of the SWCNT films were done on a 40 nm SWCNT film using a Hall Effect Measurement System model HMS 5300. The sample was previously exposed to environmental conditions overnight (laboratory air). During the measurements, nitrogen was continuously flushed inside the sample chamber and the resistance was constantly measured throughout all heating/cooling cycles. The sample was heated at 100 °C and kept at a constant temperature for 1.5 h, followed by a rapid cooling. After five consecutive heating/cooling cycles in an inert atmosphere the sample was exposed to air again for several hours. The experiment was repeated four times with similar results.

Polymer Impregnation: Epikote 828 (Resolution Nederland BV) with an equivalent weight (eqw) per epoxide group of 187 g mol^{-1} and Jeffamine D-230 (Huntsman Holland BV) with NH-eqw of 60 g mol^{-1} were used as polymer matrix. The two components were mixed at a 1:1 epoxy/amine ratio (based on epoxy group/NH equivalent) for 5 min at 700 rpm, using an RCT basic IKA magnetic stirrer, and then degassed for 3 min in a BRANSON 1510 ultrasonic cleaner. Pieces of 4×8 mm^2 were cut from the freestanding SWCNT film with the thickness of 2 µm. Each piece was placed in a silicone mold with the dimensions 5×10 mm^2, with the bottom half full with uncured polymer mixture (the SWCNT films were floating on the polymer mixture). The samples were placed in a desiccator along with an open vial of excess amine (to reduce amine evaporation from the polymer mixture), and nitrogen was flushed to remove the air from the desiccator. The samples were then subjected to a mild vacuum for 10 min. Without opening the desiccator, the upper half of the silicone molds were filled using a syringe through a septum with uncured polymer mixture, fully covering the SWCNT films. After 5 more min of vacuum, the samples were removed from the desiccator and placed in a preheated oven. They were cured at 100 °C for 4 h, with a constant nitrogen flow through the oven. A pyramid shape was cut at the top of a cross-linked sample in order to expose the 2 µm SWCNT film imbedded in the polymer. This sample was further used for ultramicrotoming. Sections of 100 and 200 nm were cut using an oscillating, 3 mm wide ultrasonic diamond knife from Diatome, with a 35° cut angle.

Supporting Information

Supporting Information is available from the Wiley Online Library or from the author.

Acknowledgements

This research forms part of the research program of the Dutch Polymer Institute (DPI), P.O. Box 902, 5600 AX Eindhoven, The Netherlands, Project No. 756 (CoCoCo).

The authors thank Mr. P.H.H. Bomans and Mr. K. Gnanasekaran for recording the TEM images.

Received: January 26, 2016
Revised: February 24, 2016
Published online: May 3, 2016

[1] M. S. Dresselhaus, G. Dresselhaus, J. C. Charlier, E. Hernandez, *Philos. Trans. A. Math. Phys. Eng. Sci.* **2004**, *362*, 2065.
[2] S. J. Tans, M. H. Devoret, H. J. Dai, A. Thess, R. E. Smalley, L. J. Geerligs, C. Dekker, *Nature* **1997**, *386*, 474.
[3] J. Bernholc, D. Brenner, M. B. Nardelli, V. Meunier, C. Roland, *Annu. Rev. Mater. Res.* **2002**, *32*, 347.
[4] J. Hone, M. C. Llaguno, M. J. Biercuk, A. T. Johnson, B. Batlogg, Z. Benes, J. E. Fischer, *Appl Phys A: Mater. Sci. Process.* **2002**, *74*, 339.
[5] M. B. Bryning, M. F. Islam, J. M. Kikkawa, A. G. Yodh, *Adv. Mater.* **2005**, *17*, 1186.
[6] I. D. Rosca, S. V. Hoa, *Carbon* **2009**, *47*, 1958.
[7] N. Grossiord, J. Loos, L. van Laake, M. Maugey, C. Zakri, C. E. Koning, A. J. Hart, *Adv. Funct. Mater.* **2008**, *18*, 3226.
[8] K. Y. Chun, Y. Oh, J. Rho, J. H. Ahn, Y. J. Kim, H. R. Choi, S. Baik, *Nat. Nanotechnol.* **2010**, *5*, 853.
[9] D. S. Hecht, A. M. Heintz, R. Lee, L. B. Hu, B. Moore, C. Cucksey, S. Risser, *Nanotechnology* **2011**, *22*, 075201.
[10] Z. C. Wu, Z. H. Chen, X. Du, J. M. Logan, J. Sippel, M. Nikolou, K. Kamaras, J. R. Reynolds, D. B. Tanner, A. F. Hebard, A. G. Rinzler, *Science* **2004**, *305*, 1273.
[11] C. A. Martin, J. K. W. Sandler, M. S. P. Shaffer, M. K. Schwarz, W. Bauhofer, K. Schulte, A. H. Windle, *Compos. Sci. Technol.* **2004**, *64*, 2309.

[12] J. M. Gonzalez-Dominguez, Y. Martinez-Rubi, A. M. Diez-Pascual, A. Anson-Casaos, M. Gomez-Fatou, B. Simard, M. T. Martinez, *Nanotechnology* **2012**, *23*, 285702.
[13] K. D. Ausman, R. Piner, O. Lourie, R. S. Ruoff, M. Korobov, *J. Phys. Chem. B* **2000**, *104*, 8911.
[14] Y. Y. Huang, E. M. Terentjev, *Polymers-Basel* **2012**, *4*, 275.
[15] N. Minami, Y. J. Kim, K. Miyashita, S. Kazaoui, B. Nalini, *Appl. Phys. Lett.* **2006**, *88*, 093123.
[16] M. J. O'Connell, P. Boul, L. M. Ericson, C. Huffman, Y. H. Wang, E. Haroz, C. Kuper, J. Tour, K. D. Ausman, R. E. Smalley, *Chem. Phys. Lett.* **2001**, *342*, 265.
[17] A. Star, J. F. Stoddart, D. Steuerman, M. Diehl, A. Boukai, E. W. Wong, X. Yang, S. W. Chung, H. Choi, J. R. Heath, *Angew. Chem. Int. Ed.* **2001**, *40*, 1721.
[18] M. Giulianini, E. R. Waclawik, J. M. Bell, M. Scarselli, P. Castrucci, M. De Crescenzi, N. Motta, *Polymers Basel* **2011**, *3*, 1433.
[19] C. Y. Li, E. T. Thostenson, T. W. Chou, *Appl. Phys. Lett.* **2007**, *91*, 223114.
[20] R. Rahman, P. Servati, *Nanotechnology* **2012**, *23*, 055703.
[21] Y. Yu, G. Song, L. Sun, *J. Appl. Phys.* **2010**, *108*, 084319.
[22] X. K. Li, F. Gittleson, M. Carmo, R. C. Sekol, A. D. Taylor, *ACS Nano* **2012**, *6*, 1347.
[23] O. A. Barsan, G. G. Hoffmann, L. G. J. van der Ven, G. de With, *Faraday Discuss.* **2014**, *173*, 365.
[24] J. Qiu, J. Terrones, J. J. Vilatela, M. E. Vickers, J. A. Elliott, A. H. Windle, *ACS Nano* **2013**, *7*, 8412.
[25] Q. Lu, G. Keskar, R. Ciocan, R. Rao, R. B. Mathur, A. M. Rao, L. L. Larcom, *J. Phys. Chem. B* **2006**, *110*, 24371.
[26] Y. B. Yao, S. D. Luo, T. Liu, *Macromolecules* **2014**, *47*, 3093.
[27] C. Laurent, E. Flahaut, A. Peigney, *Carbon* **2010**, *48*, 2994.
[28] J. E. Fischer, *Acc. Chem. Res.* **2002**, *35*, 1079.
[29] J. J. Zhao, A. Buldum, J. Han, J. P. Lu, *Nanotechnology* **2002**, *13*, 195.
[30] Y. Wang, J. T. W. Yeow, *J. Sens.* **2009**, *2009*, 24.
[31] C. H. Sun, L. C. Yin, F. Li, G. Q. Lu, H. M. Cheng, *Chem. Phys. Lett.* **2005**, *403*, 343.
[32] A. Szabados, L. P. Biro, P. R. Surjan, *Phys. Rev. B* **2006**, *73*, 195404.
[33] H. Dumlich, S. Reich, *Phys. Rev. B* **2012**, *86*, 179905.
[34] M. Kaukonen, A. Gulans, P. Havu, E. Kauppinen, *J. Comput. Chem.* **2012**, *33*, 652.
[35] T. Kim, G. Kim, W. I. Choi, Y.-K. Kwon, J.-M. Zuo, *Appl. Phys. Lett.* **2010**, *96*, 173107.
[36] A. I. Zhbanov, E. G. Pogorelov, Y. C. Chang, *ACS Nano* **2010**, *4*, 5937.
[37] E. G. Pogoreloy, A. I. Zhbanov, Y. C. Chang, S. Yang, *Langmuir* **2012**, *28*, 1276.
[38] B. Gao, Y. F. Chen, M. S. Fuhrer, D. C. Glattli, A. Bachtold, *Phys. Rev. Lett.* **2005**, *95*, 196802.
[39] C. W. Zhou, J. Kong, H. J. Dai, *Phys. Rev. Lett.* **2000**, *84*, 5604.
[40] A. Javey, J. Guo, Q. Wang, M. Lundstrom, H. J. Dai, *Nature* **2003**, *424*, 654.
[41] M. J. Biercuk, S. Ilani, C. M. Marcus, P. L. McEuen, *Top. Appl. Phys.* **2008**, *111*, 455.
[42] Y. Otsuka, Y. Naitoh, T. Matsumoto, T. Kawai, *Appl. Phys. Lett.* **2003**, *82*, 1944.
[43] A. Buldum, J. P. Lu, *Phys. Rev. B* **2001**, *63*, 161403.
[44] M. S. Fuhrer, J. Nygard, L. Shih, M. Forero, Y. G. Yoon, M. S. C. Mazzoni, H. J. Choi, J. Ihm, S. G. Louie, A. Zettl, P. L. McEuen, *Science* **2000**, *288*, 494.
[45] Q. Cao, S. J. Han, G. S. Tulevski, A. D. Franklin, W. Haensch, *ACS Nano* **2012**, *6*, 6471.
[46] Y. Woo, G. S. Duesberg, S. Roth, *Nanotechnology* **2007**, *18*.
[47] Y. Matsuda, W. Q. Deng, W. A. Goddard, *J. Phys. Chem. C* **2007**, *111*, 11113.
[48] A. Znidarsic, A. Kaskela, P. Laiho, M. Gaberscek, Y. Ohno, A. G. Nasibulin, E. I. Kauppinen, A. Hassanien, *J. Phys. Chem. C* **2013**, *117*, 13324.
[49] P. N. Nirmalraj, P. E. Lyons, S. De, J. N. Coleman, J. J. Boland, *Nano Lett.* **2009**, *9*, 3890.
[50] L. Pauling, *General Chemistry*, Dover Publications, Inc., New York **1988**.
[51] N. Tillman, A. Ulman, J. S. Schildkraut, T. L. Penner, *J. Am. Chem. Soc.* **1988**, *110*, 6136.
[52] D. J. Wold, R. Haag, M. A. Rampi, C. D. Frisbie, *J. Phys. Chem. B* **2002**, *106*, 2813.
[53] B. Ward, *M.Sc. Thesis*, Rice University, **2011**.
[54] A. B. Oskouyi, U. Sundararaj, P. Mertiny, *Materials* **2014**, *7*, 2501.
[55] N. Hu, Y. Karube, C. Yan, Z. Masuda, H. Fukunaga, *Acta Mater* **2008**, *56*, 2929.
[56] J. G. Simmons, *J. Appl. Phys.* **1963**, *34*, 1793.
[57] E. V. Buzaneva, P. Scharff, *Frontiers of Multifunctional Nanosystems*, Kluwer Academic Publishers, Dordrecht **2002**.
[58] F. M. Smits, *Bell Syst. Tech. J* **1958**, *37*, 711.